Journal of Building Engineering 43 (2021) 102549

Contents lists available at ScienceDirect

Journal of Building Engineering

journal homepage: http://www.elsevier.com/locate/jobe

An innovative timber-steel hybrid beam consisting of glulam mechanically reinforced by means of steel rod: Analytical and preliminary numerical investigations

Tianxiang Wang [a], Yue Wang [a,*], Roberto Crocetti [a], Luca Franco [b], Michael Schweigler [c], Magnus Wålinder [a]

[a] Department of Civil and Architectural Engineering, KTH Royal Institute of Technology, SE-100 44, Sweden
[b] Dipartimento di Culture del Progetto, Univiersità IUAV di Venezia, Dorsoduro 2206, 30123, Venice, Italy
[c] Department of Building Technology, Linnaeus University, Universitetsplatsen 1, 35195, Växjö, Sweden

ARTICLE INFO

Keywords:
Hybrid structure
Mechanical connection
Shear key
Timber-steel hybrid beam
Analytical model
Numerical analysis
Retrofitting techniques

ABSTRACT

There is an increasing interest in large-dimensional timber structural elements within the construction sector in order to fulfil the combined demand of sustainability, open spaces and architectural flexibility. Current timber technology allows for efficient production of long-size beams, but many problems are related to their overall high costs due to difficulties in transportation, manufacturing on site and handling during the mounting phase. Hence, the aim of this work is to propose and study an innovative timber-steel hybrid structural element composed of shorter pieces of beams connected and reinforced by means of a system consisting of steel shear keys and steel rods. The small timber elements and steel devices can be prefabricated with low costs and easily assembled into large elements at the construction sites. The proposed system can also be used for retrofitting of existing timber members when it is necessary to increase their strength, stiffness and ductility. The structural behavior of the proposed system was therefore studied both as a connection and as a retrofitting technique, which were analyzed via two types of hybrid beams, one with a splice at mid-span and one without, separately. A simple glulam beam with the same geometrical characteristics of the two hybrid structures was also investigated for the comparison of the structural behavior. The analytical results show that the hybrid beams with and without splice have both obtained significant increasement in the stiffness, strength and ductility. The numerical analyses are limited in the elastic stage due to the elastic mechanical properties assigned to the structural components. The numerical results show good agreement with the analytical ones for each type of beam in terms of the stiffness in the elastic stage. Finally, the influence of the parameters such as the distance between shear keys, slip modulus of shear keys and diameter of rod, on the structural behavior of hybrid beams is discussed in this paper.

1. Introduction

There is an increasing interest and demand within the construction sector to combine the benefits of mineral-based building materials with the benefits of bio-based ones [21]. Some studies have been conducted in the field of timber-based hybrid structures. Layered timber-concrete composite (TCC) structures, which in most cases utilize concrete in compression and timber in tension, provide an innovative method to the flooring system [1,5,18]. Timber-steel hybrid structures (e.g. steel frames with an infilled wooden shear wall) attract lower forces during an earthquake and achieve good seismic performance due to the high strength-to-weight ratio of timber and the ductility behavior of steel [19,34].

In recent years, large-dimensional timber structural elements are highly demanded for the construction of high-rise timber buildings as well as large-span structures [26]. However, long-span wooden products are not easy to handle during transportation and erection phases, making them therefore particularly expensive [6]. In order to find a solution to these problems, an innovative timber-steel hybrid member composed of timber beams mechanically jointed together through steel shear keys and rods is proposed in this work.

Two types of connections, namely adhesive or mechanical connections, are usually adopted to connect shorter elements in order to create

* Corresponding author.
E-mail address: yue4@kth.se (Y. Wang).

https://doi.org/10.1016/j.jobe.2021.102549
Received 16 September 2020; Received in revised form 7 April 2021; Accepted 13 April 2021
Available online 16 April 2021

longer spans. The advantage of the former is mainly the high composite efficiency and economy. On the other hand, adhesive connections have the main drawback of being difficult to assemble on site, since the adhesive joints need an accurate control of moisture and temperature condition [27]. Mechanical connections, on the other hand, have in general lower strength and stiffness than adhesive connections [32]. However, they have the advantage of easy installation on site. Moreover, considering the end-of-life (EOL) cycle of the building, mechanical connections allow for more flexible and less expensive unmounting processes with mostly re-useable components, which is beneficial for reducing waste and promoting the circular economy [29].

Shear key connections produce partial composite action, meaning that the slip between the connected parts is non-negligible and the strain distribution is not continuous along the composite cross-section [17,22,30]. However, apart from adhesive connections, the shear-key connection is one of the most efficient type among the mechanical connections to create composite actions in timber-based structures [4,33].

Shear keys have been mainly studied in wood-concrete composite beams, for example in Ref. [24]. Here, the authors analyzed how effectively the shear key can resist the interlayer slip between wood and concrete layer. An average composite efficiency of over 80% was reached in full-size test specimens when loaded under four-point bending. The most common failure was due to the interaction of bending and tension at mid-span starting from the bottom of the wood member. Mechanically laminated timber beams using different types of wooden shear keys were studied in Ref. [25]. Here, the authors developed a theoretical interlayer slip model under linear elastic hypothesis to investigate the stiffness of the wooden shear key. Both small and full-scale tests were performed to validate the analytical model. Results showed that the stiffness from the interlayer slip model was slightly larger than the one obtained experimentally. The authors concluded that the overestimation might be due to the nonlinear behavior of materials in the test neglected by the linear model. Shear keys made of beech were studied for the connection between CLT elements in Ref. [28], where LVL shear keys with different slenderness ratios loaded perpendicular to the grain were investigated through experimental tests. It was found that for shear keys with a low slenderness ratio the load-bearing capacity is dependent on the embedment length into the CLT element, whereas for the shear key with a higher slenderness ratio the load-deformation capacity is mainly influenced by the compression stress perpendicular to the grain.

Although some studies regarding the shear key connection have been carried out in the past, current design standards do not provide adequate guidelines for designing shear key connections [2,12,13,25,31].

In this paper, an innovative timber-steel hybrid system for mechanical connection and reinforcement of glulam is presented. The structural behavior of this hybrid system is analyzed through both analytical and numerical models considering a four-point loading condition. Further, parametric analyses are carried out in order to study the behavior of the system when different mechanical parameters are varied.

2. Materials and methods

2.1. Description of the hybrid structural system

In order to study the hybrid structural system as a retrofitting technique, a monolithic glulam beam with symmetrical notch positions to the mid-span is pre-produced. Then, shear connectors are inserted into the notches at the bottom of glulam and a steel rod assembles these connectors, as well as the glulam beam, together. The connectors installed on the glulam beam act as shear keys and the steel rod acts as reinforcement at the bottom (Fig. 1a). This type of beam is annotated as hybrid beam without splice.

Another type of hybrid beam is also studied for the purpose of creating longer spans from shorter elements. Differently from the hybrid beam without splice in Fig. 1.a, two half-length glulam beams are jointed together at mid-span by two steel plates, annotated as splice in Fig. 1.b. The steel plates are used on the upper and contacting surface to avoid penetration of wood fibers at compressed head-to-head interface [15]. This type of beam is annotated as hybrid beam with a splice at mid-span.

Each shear key consists of one solid steel component and one steel plate (Fig. 2). The solid steel component shown in Fig. 2.a, consists of two parts: an upper part which is inserted into the notch at the bottom of the timber beam (annotated as tooth) and a lower part (annotated as plinth), which is screwed to the bottom side of the timber beam. For each shear key eight fully threaded screws are employed (Fig. 2.b and Fig. 2c). Six screws (with an outer diameter of 9 mm and a length of 200 mm) are inserted into predrilled holes with diameters of 10 mm on the plinth of shear key and are activated in tension when the shear key tends to rotate due to the eccentricity of the steel rod. The other two screws (with an outer diameter of 9 mm and a length of 160 mm) are not inserted through the shear key; instead, their heads are placed on the bottom surface of the timber element: they only serve as local rein-

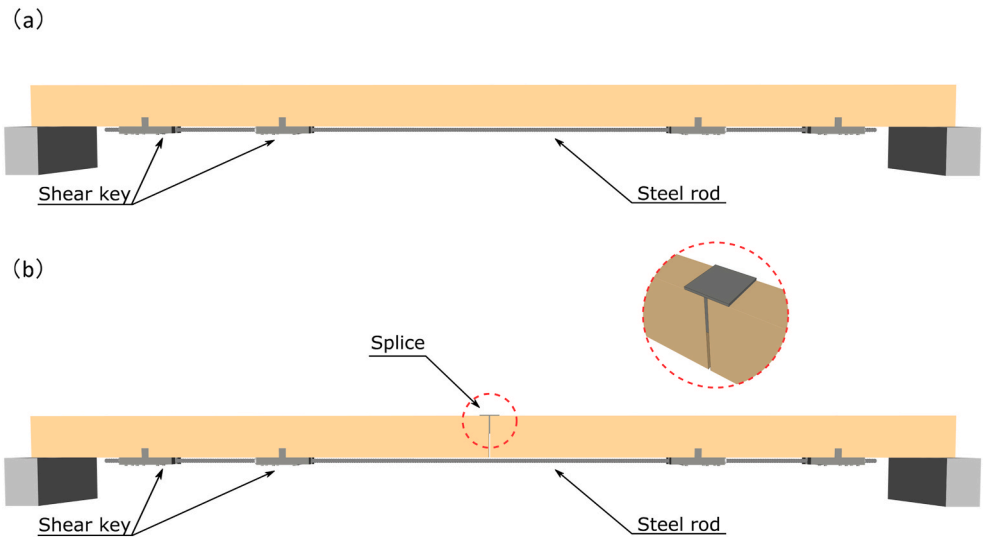

Fig. 1. A general view of the innovative hybrid structural system (a) the hybrid beam without splice and (b) the hybrid beam with a splice at mid-span.(Please see online version for colors.)

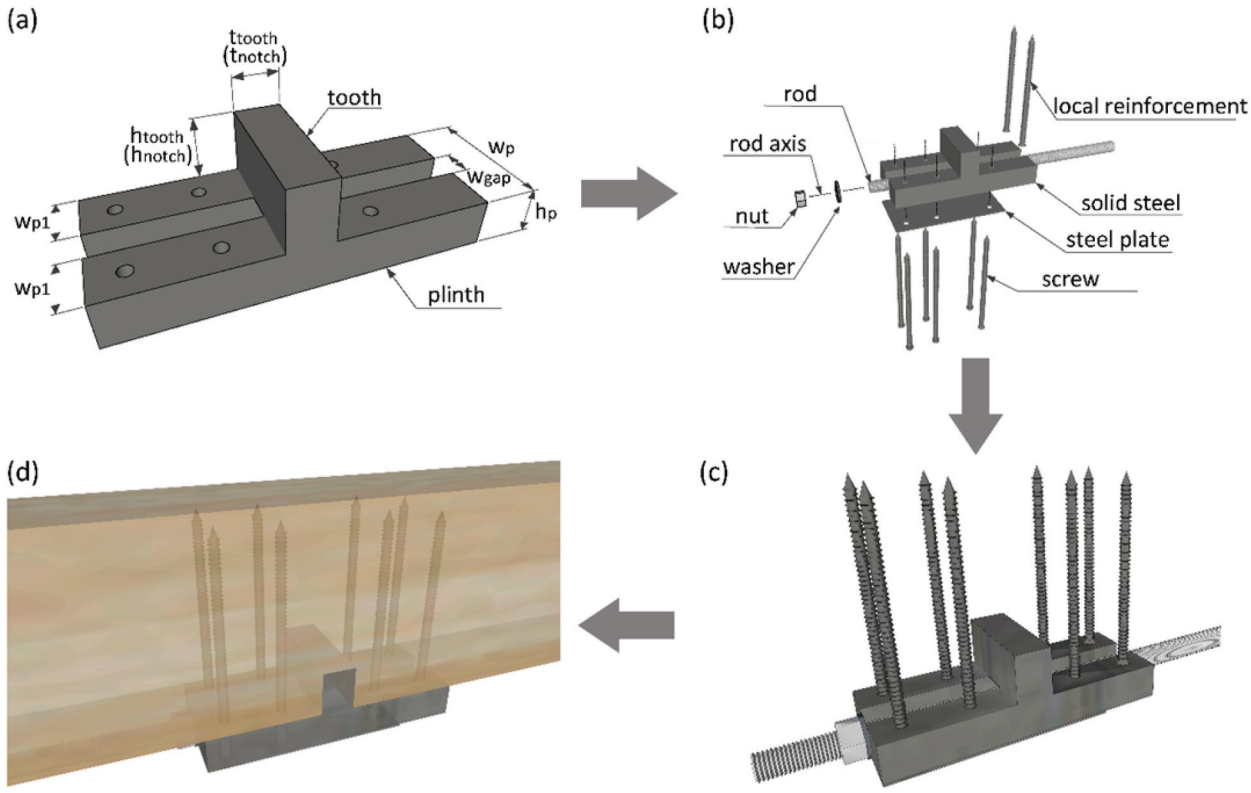

Fig. 2. Components and assembly process of shear key connections (a) configuration of solid steel, (b) components of the shear key, (c) assembly process of the shear key and (d) the assembled shear key connection with glulam beam.(Please see online version for colors.)

forcement to improve the stiffness and strength of timber perpendicular to the grain. When the shear key is assembled into the glulam beam, the rod can be anchored through the gap of the plinth of the shear key by nuts and washers. Finally, as shown in Fig. 2.d, the assembly process is complete. The glulam beam is reinforced by the steel rod with the connection of the steel shear keys.

2.2. Configurations of the investigated beams

The proposed hybrid structural system was therefore investigated for both the possible usages, as reinforcement system for existing timber beams analyzing a hybrid beam without splice, and as connection technique to create longer beams from shorter pieces analyzing a hybrid beam composed of two timber joists with a splice at mid-span. The effectiveness of both the analyzed system configurations was evaluated by comparing the outcomes of these two analyses with the correspondent performances of a simple glulam beam with the same geometrical characteristics of the two hybrid structures. In general, three types of beams were investigated in this study: (a) simple glulam beam, (b) hybrid beam without splice and (c) hybrid beam with a splice at mid-span (see Fig. 3).

2.2.1. Simple glulam beam (Fig. 3 a) (labeled as SGB)

As a reference for comparison with the investigated hybrid beams, a simple glulam beam GL 30c with a width of 90 mm, a height of 180 mm and a length of 4200 mm was analyzed. The distance between the two supports is 4000 mm.

2.2.2. Hybrid beam without splice (Fig. 3 b) (labeled as HB)

A glulam beam with the same dimension as the simple glulam beam is reinforced by means of an M16 steel rod with strength grade 8.8 (Yielding strength f_y = 640 MPa). Four notches are located at the bottom of the glulam beam with dimensions 90 mm (width), 40 mm (height) and 30 mm (length) and at a distance of 0.5 m, 1.1 m, 2.9 m and 3.5 m from the supports. The notches are needed for the installation of the shear key anchoring system. As for the configuration of the shear key shown in Fig. 2.a, the inserted part of the shear key, annotated as tooth, has the same width with the glulam beam, which is 90 mm. The thickness t_{tooth} is 30 mm and the depth h_{tooth} equals 40 mm. The plinth of shear key has a length of 100 mm on each side, a depth h_p of 30 mm and a width w_p of 90 mm. Two solid parts of plinth have equal width w_{p1}, which is 33 mm, thus a 24 mm (w_{gap}) wide gap is left in between for the steel rod to go through.

2.2.3. Hybrid beam with a splice at mid-span (Fig. 3c) (labeled as HBS)

Differently from the hybrid beam without splice, the timber beam in this case is not monolithic, but it consists of two separate 2.1 m-long glulam beams. Therefore, this type of beam presents a splice at mid-span. For real applications, a steel plate with a height of 75 mm and a thickness of 6 mm is installed on the upper part of the contact interface to avoid penetration of wood fibers due to compression of end-grain contact interface [15].

2.3. Analytical models

Analytical models for the investigated beams were introduced in this section. For both types of hybrid beams, global load-deformation behavior and local behavior in the vicinity of the shear key connections were studied in order to determine the structural behavior until failure. Moreover, a comparison between each type of beam was carried out in the elastic stage, under the same external load of 10 kN at each one-third point of the glulam beam.

2.3.1. Mechanical properties

Mechanical properties of glulam timber and steel rod, i.e. elastic modulus, strength, and the corresponding yielding and plastic strains

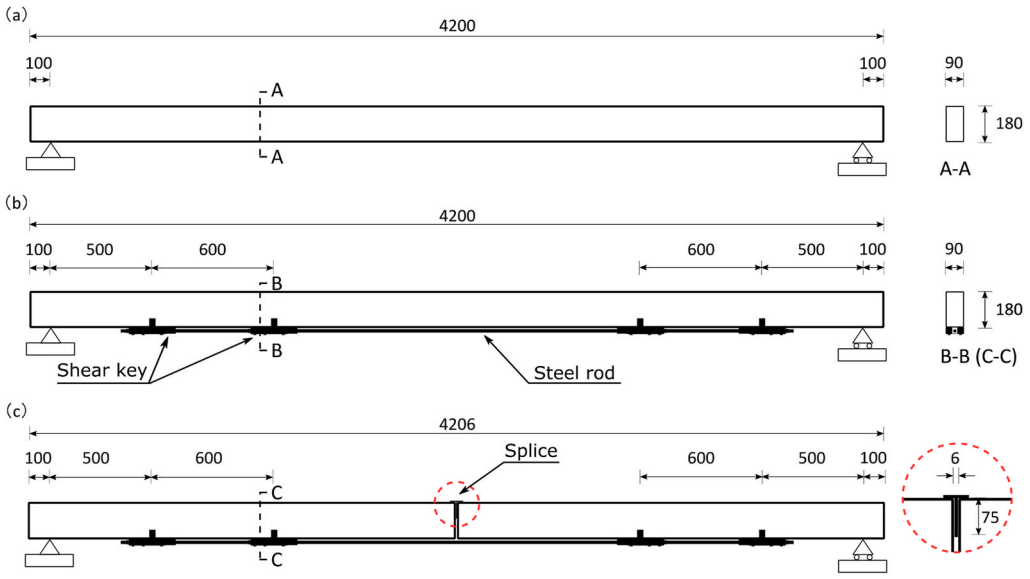

Fig. 3. Geometrical configurations of the analyzed beams: (a) simple glulam beam, (b) hybrid beam without splice and (c) hybrid beam with a splice at mid-span. (unit: mm).(Please see online version for colors.)

were determined for analytical studies according to Ref. [7]. The steel shear key was assigned the same material properties as the steel rod with strength grade 8.8.

For timber material, the probabilistic model [20] was employed to calculate the mean strength values from their characteristic values (See Table 1).

The maximum elastic strain was calculated according to Hook's law. The maximum plastic strain of wood in compression parallel to the grain and the maximum tensile plastic strain of rod are assumed to be three times the maximum elastic strain [7].

2.3.2. Simple glulam beam (SGB)

The deflections were determined using the classical Euler-Bernoulli beam theory under four-point bending loading.

2.3.3. Hybrid beam without splice (HB)

(a) Global load-deformation behavior

The second order linear differential equation with constant coefficients that describes the behavior of beams with partial composite action is:

$$N_1'' - \omega^2 \cdot N_1(x) = C \cdot M(x) \tag{1}$$

Table 1
Material properties of glulam GL 30c according to Refs. [7,20].

	Characteristic value (MPa) (MPa)	COV	Distribution function	Mean value (MPa)
Bending strength	$f_{m,k}$ = 30.0	0.15	Lognormal	$f_{m,m}$ = 38.2
Tensile strength parallel to the grain	$f_{t,0,k}$ = 19.5	0.18	Lognormal	$f_{t,0,m}$ = 26.0
Compressive strength parallel to the grain	$f_{c,0,k}$ = 24.5	0.12	Lognormal	$f_{c,0,m}$ = 29.8
Compressive strength perpendicular to the grain	$f_{c,90,k}$ = 2.5	0.10	Normal	$f_{c,90,m}$ = 9.0
Shear strength	$f_{v,k}$ = 3.5	0.15	Lognormal	$f_{v,m}$ = 4.5

Note: the mean value of compressive strength perpendicular to the grain, $f_{c,90,m}$, takes into consideration both the small bearing area and the local reinforcement exerted by the screws [11].

where,

$$\omega = \sqrt{\frac{k_{ser}}{s} \cdot \left(\frac{1}{E_1 \cdot A_1} + \frac{1}{E_2 \cdot A_2} + \frac{h_t^2}{E_1 \cdot I_1 + E_2 \cdot I_2} \right)} \tag{2}$$

$$C = \frac{k_{ser} \cdot d}{s} \cdot \left(\frac{1}{E_1 \cdot I_1 + E_2 \cdot I_2} \right) \tag{3}$$

where ω and C are the composite cross-sectional and material constants respectively; $N_1(x)$ is the internal axial force in layer one on the section located at the longitudinal position x; $M(x)$ is the external bending moment acting on the composite cross-section at the longitudinal position x; s is the (constant) spacing of inter-layer connections (in the specific case, shear keys); E_i, I_i,A_i (i = 1, 2) are the elastic modulus, the second moment of inertia and the cross-sectional area of the i-th layer respectively; h_t is the vertical distance between the axes of the two layers (in the specific investigated case, the steel rod was positioned aligned with the barycenter of the steel plinth of the shear key); k_{ser} is the slip modulus of shear key due to the contact pressure in the longitudinal direction between the tooth of the shear key and the timber notch. For notch depth deeper than 3.0 cm a design value of the slip modulus 1500 kN/mm per meter beam width is suggested for the shear connection between timber and concrete [9]. The same criterion has been assumed for the connection between timber notch and steel shear keys in the investigated hybrid system. Since the timber component of the hybrid beam has a notch depth of 4.0 cm and a section width of 90 mm, a design value of the slip modulusk_{ser} = 1500 kN/mm/m ∗0.09 m =135 kN/mm was used.

(1) was solved by means of two analytical methods, namely: the partial composite method (henceforth labeled as "PC method") [7] and the gamma method (henceforth labeled as "γ method") (EN 1995-1-1:2004, 2004). The following assumptions were applied in both methods:

- Euler-Bernoulli beam theory was assumed;
- linear elasticity was assumed;
- small displacement theory was assumed;
- shear deformations within each component were neglected;
- constant connector spacing was assumed (in the specific investigated case each hybrid beam has 4 shear keys with a constant spacing of 1 m);

- no interlayer separation was assumed (therefore both components have equal deflection and radius of curvature in each corresponding section); and
- rheological behavior, the effects of swelling and shrinkage of timber were neglected.

The main difference between the two methods is that the PC method takes the real load condition into consideration, whereas the γ -method, as a simplified method, assumes that the load has a near-half-sinusoidal distribution over the beam span.

According to the PC method, the internal bending moment acting in layer one and two at the longitudinal position x, $M_1(x)$and $M_2(x)$ can be derived by (4) and (5), and the beam deflection at the longitudinal position x, $\omega(x)$, can be derived by (6).

$$M_1(x) = \frac{I_1}{I_1 + I_2} \cdot \left(M(x) + h_t \cdot N_1(x)\right) \tag{4}$$

$$M_2(x) = \frac{I_2}{I_1 + I_2} \cdot \left(M(x) + h_t \cdot N_1(x)\right) \tag{5}$$

$$\omega(x) = \omega_{fca}(x) - \frac{C}{k_{core} \cdot \omega^2} \cdot N_1(x) + D_3 \cdot x + D_4 \tag{6}$$

where $\omega_{fca}(x)$ is the bending deflection in full composite action at the longitudinal position x; $k_{core} = k_{ser}/s$ is the smeared out stiffness; D_3, D_4 is the integration constants (zero in this case).

(b) Local behavior of the shear key connection

In order to verify if there is any risk for local failure in the vicinity of the shear key connections, the highest axial force transferred from the rod to shear key under global failure F_{ax} was utilized for the local check. Three possible local failure modes (Fig. 4) were verified for both hybrid beams without splice and with a splice at mid-span, and they are:

I compressive failure parallel to the grain on the side surface of the notch in glulam;
II shear failure around the notch along the grain in glulam, where the influence length of shear stress was considered to be eight times the height of the notch [9]; and
III withdrawal failure of the screws in tension.

Regarding the third local failure mode, the withdrawal force acting on each screw $F_{ax,Ed}$ is:

$$F_{ax,Ed} = \frac{F_{ax} \cdot h_{lh}}{n \cdot h_{lv}} \tag{7}$$

where F_{ax} is the highest axial force transferred from the rod to shear key under global failure; h_{lh} is the lever arm between horizontal forces, and it is assumed to be $h_{lh} = \left(h_{notch} + h_p\right)/2$; h_{notch} and h_p are the height of notch and of the plinth of the shear key respectively; n is the number of screws in tension; h_{lv} is the lever arm between vertical forces which was taken from the resultant force in the left part of the plinth of the shear key to that in the right part.

The characteristic withdrawal capacity for the screw inserted perpendicular to the grain $F_{ax,Rk}$ is derived according to the technical approval [14]. The corresponding design withdrawal capacity $F_{ax,Rd}$ is (EN 1995-1-1:2004, 2004):

$$F_{ax,Rd} = \frac{k_{mod} \cdot F_{ax,Rk}}{\gamma_M} \tag{8}$$

where k_{mod} is the modification factor and γ_M is the partial factor for connections.

2.3.4. Hybrid beam with a splice at mid-span (HBS)

An ad-hoc mechanics-based analytical model for HBS has been developed and presented in Ref. [16]. The glulam component, the steel rod and the shear keys were modeled as beam-type linear elements, truss-type linear element and rigid elements, respectively. The shear keys were connected to the upper glulam beams and the lower steel rod by means of discrete spring elements with the slip modulus k_{ser}. The mechanical behavior around mid-span was represented by a hinge located at the resultant compressive force. Some basic assumptions were made for the investigation of the mechanical model, among which:

- Euler-Bernoulli beam theory was assumed;
- small displacement theory was assumed;
- elastic behavior of the material was assumed for the calculation of forces and deflection;
- elasto-plastic behavior of glulam and steel rod was assumed only for the calculation of the position of the neutral axis with respect to the compressive zone in glulam;
- shear deformations within each component were neglected; and
- rheological behavior, the effects of swelling and shrinkage of timber were neglected.

The analytical model is able to predict both the internal force and deflections for each component.

2.4. Numerical models

2.4.1. General description

Numerical analyses were performed with commercial finite element software Abaqus (Simulia, USA). Planar 2D models were created for investigation of forces and deflections on both global-structure and single

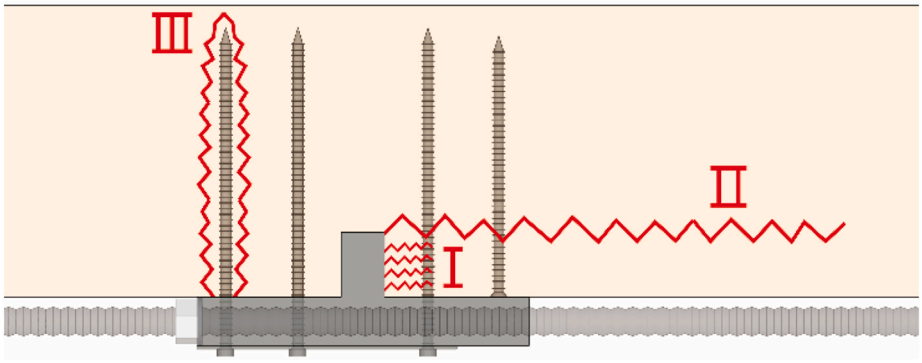

Fig. 4. Possible local failure modes in the vicinity of the shear keys: (I) compressive failure parallel to the grain on the side surface of the notch in glulam, (II) shear failure around the notch along the grain in glulam and (III) withdrawal failure of the screws in tension.(Please see online version for colors.)

component level. The glulam component, the steel rod and the shear keys were modeled as beam-type linear elements, truss-type linear element and rigid elements, respectively. All the structural components were assigned with linear elastic material properties. The comparison between each type of numerical model was under the same four-point loading scheme with an external load of 10 kN placed at each one-third span point.

2.4.2. Material properties

Isotropic elastic material properties were assigned to the steel rod.

The glued-laminated timber is usually characterized as an orthotropic material. Yet the mathematical modeling of the glulam beams can be greatly simplified by considering the material to be transversally isotropic [3,8]. Thus, in this numerical analysis, glulam beam was modeled with identical stiffness and strength properties in the radial and tangential directions. The properties assigned for glulam include density ρ, elastic modulus E_{ij}, Poisson's ratio ν_{ij} and shear modulus G_{ij}. Class of glulam GL 30c is assumed, and the mechanical parameters (see Table 2) have been derived according to Ref. [7] for the mean values of density, elastic modulus and shear modulus and [10] for Poisson's ratios.

2.4.3. Modeling process

Models for each type of beam are schematically presented in Fig. 5. For hybrid beams the shear key was modeled with a fictitious rigid beam element, which was vertically connected to the glulam beam axis. The fictitious, rigid vertical element was defined as rigid body, tied to the glulam beam, and thus was always aligned perpendicular to the glulam beam axis. Regarding the interaction between shear key and rod, a spring was firstly created connecting the two components at the location of the rod. Then, rigid contact was assigned for translational degrees of freedom (DOFs) in transversal directions and all the rotational DOFs for the spring. Linear elastic contact with the local stiffness of shear key $k_{ser}$was defined for the spring in the longitudinal direction.

The mid-span splice of the beam shown in Fig. 5.c was modeled with an eccentric hinge connected to the axis of the timber component through rigid beam elements. The hinge was placed to form an eccentricity which corresponds to the point of action of the resultant compressive force, determined by assuming linearly distributed stresses at mid-span timber interface. An eccentricity value of 65 mm was adopted for the numerical model of the hybrid beam with splice.

The common parts of the modeling process for all types of beams were: (a) boundary conditions: simply supported, (b) load condition: four-point bending, and (c) mesh element type and size: beam element type (B22 in ABAQUS/CAE 2018, Simulia, USA and mesh size 0.02 m for glulam; truss element type (T2D2 in ABAQUS/CAE 2018, Simulia, USA) for rod; and discrete rigid element (R2D2 in ABAQUS/CAE 2018, Simulia, USA) for rigid elements at shear keys and splice at mid-span.

Table 2
Material properties of glulam GL 30c for numerical analysis.

ρ(kg/m3)	E_{11} (MPa)	E_{22} (MPa)	E_{33} (MPa)	ν_{12}
430	13000	300	300	0.219
ν_{13}	ν_{23}	G_{12} (MPa)	G_{13} (MPa)	G_{23} (MPa)
0.219	0.582	650	650	65

Note: subscripts i,j =1, 2, 3 used for the material properties in Table 2, stand for the principal material directions. Axis 1 is aligned along the grain, while axis 2 and 3 are defined according to the convention of the right-handed coordinate system. Additionally, the rolling shear modulus $G_{23}$was assumed to be one-tenth of the shear modulus G_{12} and G_{13} according to Ref. [23].

2.4.4. Parametric analysis

In this study a parametric analysis on the main characteristics that influence the structural response of the novel hybrid system was performed in order to study and improve its mechanical performance. The studied parameters are (a) the position of the shear keys in the longitudinal direction of the beam, (b) the slip modulus of shear key and (c) the diameter of the rod. All the other mechanical and geometrical parameters were kept constant. The load was constantly set as 10 kN at each one-third point of glulam beam. For the first studied parameter, only deflection was compared, while for the latter two parameters, effects on axial forces in glulam beams and the rod, force distribution in each shear key, deflections in glulam were investigated.

(a) The position of the shear keys

Considering that the influence length of local shear failure around shear key along the longitudinal direction was assumed as eight times

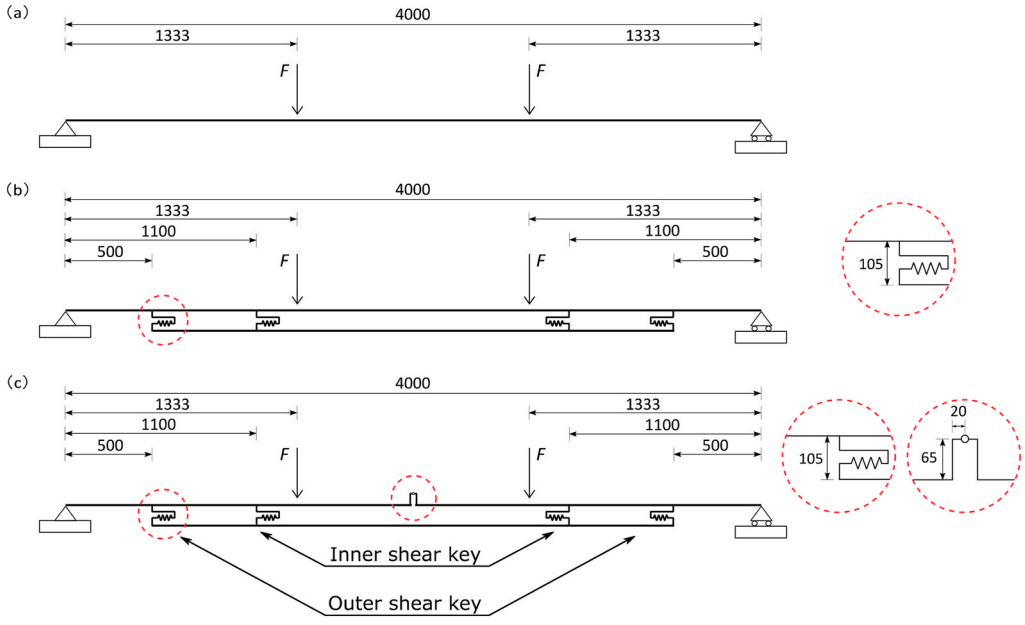

Fig. 5. Loading and geometrical configurations of the investigated beam models: (a) simple glulam beam (SGB), (b) hybrid beam without splice (HB) and (c) hybrid beam with a splice at mid-span (HBS). (unit: mm).(Please see online version for colors.)

the depth of notch [9], the distance between the inner and outer shear key (including the length of notch) should not be less than 0.35 m.

For hybrid beam without splice, the horizontal force F taken by each shear connector (in N) is equal to:

$$F = v \cdot s \tag{9}$$

where v is the shear flow in the glulam (in N/mm) and s is the spacing of connector (in mm). Within the part between two external loads, the shear flow equals zero since the bending moment is constant in each structural component. Therefore, it is more efficient to arrange the shear keys among the two sided one-third parts of the beam.

For hybrid beam with a splice at mid-span, the force taken by each shear key is the function of relative stiffness (e.g. the slip modulus of shear key, the stiffness of glulam and rod) and is due to lack of material continuity [16]. The specific load-resistant mechanism is explained in detail in Section 3.2. If the inner shear key is positioned in the middle one-third part, the stiffness of the hybrid system would not necessarily decrease. However, the decreased axial force in the part between the external load and the inner shear key would lead to a higher bending moment in the glulam, thereby reducing the load-bearing capacity of the hybrid system.

During this parametric study, for both types of hybrid beams, the location of the outer shear keys (measured from the closest support) was varied between 0.3 m and 0.8 m with an interval of 0.1 m. The location of the inner ones (measured from the closest support) was varied between 0.7 m and 1.2 m with the same interval.

(b) Slip modulus of shear key

As mentioned in Section 2.3, the design value of the local spring stiffness for the shear keys k_{ser} =135 kN/mm is based on timber-concrete notched connection tests. Its application to timber-steel hybrid structures could be questioned. However, due to the lack of more reasonable input data, k_{ser} was taken as a reasonable estimation in this study. In order to determine if this uncertainty of the value assigned to this parameter significantly affects the final obtained results, a sensitivity analysis was carried out varying the parameter within the range from 5 kN/mm to 205 kN/mm with an interval value of 10 kN/mm.

(c) Diameter of the rod

The diameter of rod d_{rod} changed from 2 mm to 30 mm with an interval value of 2 mm.

It is worth mentioning that the change of the upper three parameters, i.e. the position of the shear keys, slip modulus of shear key and diameter of the rod, only took place in this parametric study. For the rest analysis, the position of the outer and inner shear keys (0.5 m and 1.1 m from the supports), slip modulus of 135 kN/mm and M16 rod were always used.

Table 3
Comparison of analytical results under 10 kN external load at each third-point of the beam.

Type	SGB	HB		HBS
		PC Method	γ Method	
Axial force in the rod (kN)	–	48.7	47.0	73.6
Bending moment in glulam at mid-span (kNm)	13.3	8.2	8.4	5.6*
The maximum deflection in glulam (mm)	40.0	25.1	25.1	32.3

Note: the value with asterisk in Table 3 shows the bending moment acting on the mid-depth of the end grain glulam cross-section in HBS at mid-span, due to the eccentricity of the resultant compressive force.

3. Results and discussion

3.1. Analytical results

The structural behavior of the investigated beams (see Fig. 3) was firstly compared under the same external load of 10 kN at each one-third point of the glulam beam. Results based on analytical calculations were compared for each type of beam and analytical calculation method, as shown in Table 3. It is shown that the simple glulam beam (SGB) has the highest bending moment and deflection among the three types of investigated beams. Compared with the hybrid beam without splice (HB), the hybrid beam with splice (HBS) has higher axial force and deflection in the glulam component.

Fig. 6 shows a schematic representation of strain and stress distributions for the hybrid beams when the global failure occurs. For the hybrid beams, failure is defined when the maximum elastic strain in any hybrid beam element has occurred. For HB, the section at mid-span was checked. Yielding of glulam in compression parallel to the grain occurs when the load is 14.8 kN (Fig. 6.a). For HBS, sections at mid-span and around the inner shear key were both checked. The hybrid structure HBS fails because of the yielding of the rod in tension between the two internal shear keys when a load of 16.5 kN is applied (Fig. 6.b). The highest axial forces transferred to the shear keys under global failure were used for local checks. It is worth noting that none of the possible local failure modes happens before the global failure, and this is important for the hybrid beams in order to guarantee a ductile failure due to yielding of glulam in compression parallel to the grain or yielding of the steel rod. Table 4 reports a summary of the structural behaviors of the three types of beams under failure.

3.2. Discussion of analytical results

The bending moment caused by the external load is taken by the composite structure through two different resisting mechanisms, namely: (a) the axial force in glulam (or in the steel rod) times the lever arm and (b) the bending moment in glulam. The rod has no bending stiffness; therefore, it does not contribute to take any direct bending

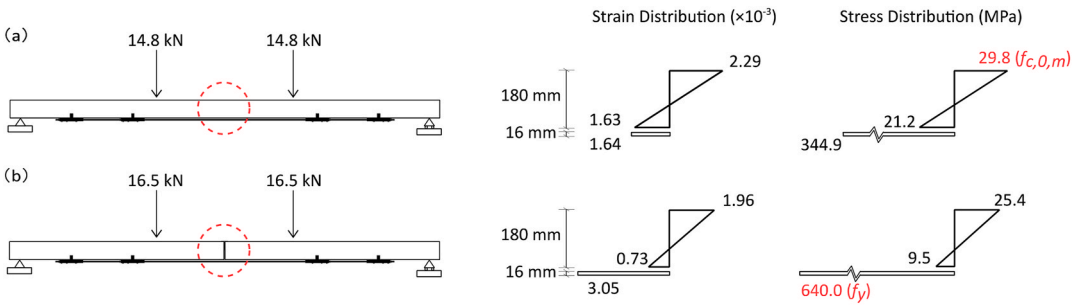

Fig. 6. Strain and stress distributions along the cross section at mid-span, (a) for HB and (b) for HBS.(Please see online version for colors.)

Table 4
Comparison of analytical results when failure is reached on each type of beam.

Type	SGB	HB		HBS
		PC Method	γ Method	
The external load at each third-point (kN)	13.9	14.8	14.8	16.5
Axial force in the rod (kN)	–	71.9	69.4	128.7
The maximum bending moment in glulam (kNm)	18.6	12.1	12.4	8.5
The maximum deflection in glulam (mm)	55.7	37.1	37.0	56.9
Failure mode	Bending failure	Yielding of glulam in compression parallel to the grain		Yielding of rod in tension

moment. As can be seen in Table 3, the external load is fully taken by the bending moment for SGB whereas the glulam beam accounts less contribution for the hybrid beams HB and HBS. The difference of axial force and bending moment between the two hybrid beams is due to the fact that the glulam part of HBS is lack of continuity at the mid-section, therefore only the timber-steel composite section consists the resistant system. On the other hand, HB is expected to carry the external load by its glulam part solely, and the composite action is only an extra-resistant contribution that works in parallel with the other.

In addition, the secant stiffness of each type of beam was compared based on the results in Table 3. It is found that SGB is the least stiff one of the three studied systems. HBS and HB, with lower deflection in glulam, are both stiffer than SGB. The high stiffness of the steel components, especially the steel rod, remarkably improve the stiffness of the hybrid beams. For HB and HBS, when the external loads induce the bending moment, the high tensile stress that should have been taken by the lower part of the glulam is yet absorbed by the steel rod, leading to a lower bending moment in the glulam beam (which is the main contributor to the deflection) compared to SGB. Moreover, for HB, highly similar results can be observed from both the PC method and the γ method. This is due to the fact that the bending moment diagram of a simply supported beam subjected to two equal concentrated loads is similar to the moment diagram of a similar beam subjected to sinusoidal shaped load, as assumed in the γ method.

The strain and stress distributions along the cross section of the hybrid beams were reported in Fig. 6 when failure has occurred. Only slight discontinuity of strains can be observed between the glulam and the rod for HB, indicating that this hybrid structure presents nearly a full composite action. This means that the assumed slip modulus of the shear key is considerably high. The effective magnitude of the local shear key stiffness needs, however, to be verified by means of appropriate experimental tests.

For HBS, both the cross section at mid-span and the cross section at the inner shear key were checked for strain and stress, since in these sections the highest axial forces and the highest bending moment were computed, as shown in Fig. 7.

Table 4 compares the structural behavior of the three investigated beams at failure. Brittle bending failure is expected for SGB while the hybrid beams HB and HBS behave in a ductile manner. In the hybrid beams, in fact, failure occurs either due to a) yielding of glulam in compression parallel to the grain or b) tension failure of the steel rod or c) a combination of a) and b). HBS has the highest bearing capacity owing to the high utilization of the strength of the steel rod. However, both types of hybrid beams could continue to withstand external load due to load redistribution in the plastic stage. It is possible that HB has higher load-bearing capacity in the real ultimate limit stage. Further analysis regarding the redistribution phenomenon should be conducted in the future. Nevertheless, as shown in Table 4, HBS has lower serviceability performance with higher deflections (approximately 1/70 of the beam span) due to the different loading resisting mechanism that develops a high amount of rigid deflection contribution [16]. Thus, the issue in the serviceability limit state is more critical for HBS.

3.3. Numerical results

Planar 2D numerical models were created for the investigations of three types of beams, i.e. SGB, HB and HBS (see Fig. 5). Results based on numerical analysis under the same external load, i.e. 10 kN at each one-third point of glulam beam are listed in Table 5. It is noticeable that HBS has the highest axial force in the rod and transferred to the shear keys while HB has the lowest deflection in both glulam and rod among the three types of investigated beams. Fig. 7 shows axial force, bending moment and deflection diagrams for the three types of beams. It is shown in the axial force diagram (Fig. 7.a) and bending moment diagram (Fig. 7.b) that there are some sudden changes of axial force in the rod and bending moment in glulam in the positions of 0.5 m, 1.1 m, 2.9 m and 3.5 m from the support where shear keys are located at for HB and HBS. There is clearly no axial force for SGB and this type of beam has the highest deflection compared to the hybrid beams under the same external load.

Parameter analysis was performed to study the influence of the main characteristics on the structural behavior of the hybrid beams, i.e. HB and HBS. Results of the parametric studies were compared under the constant external load, i.e. 10 kN at each third-point of the beam. Firstly, the effect of different longitudinal positions of the shear keys on the deflections in glulam at mid-span was investigated. Table 6 shows that HB reaches the minimum deflection at mid-span with a value of 26.6 mm when the outer and inner shear keys are located at 0.3 m and

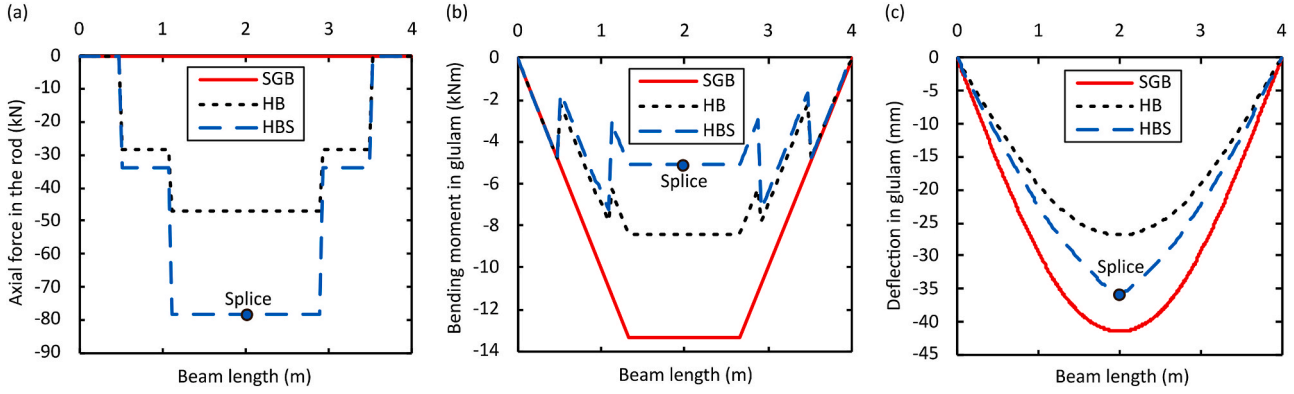

Fig. 7. (a) Axial force diagram, (b) Bending moment diagram and (c) Deflection diagram of the investigated beams based on numerical results.(Please see online version for colors.)

Table 5
Comparison of numerical results under 10 kN external load at each third-point of the beam.

Type	SGB	HB	HBS
Axial force in the rod (kN)	–	47.1	78.4
Bending moment in glulam at mid-span (kNm)	13.3	8.4	5.1*
The maximum deflection in glulam (mm)	41.4	26.8	36.2
The maximum deflection in the rod (mm)	–	20.6	24.3
Force transferred to the outer shear key (kN)	–	28.4	33.7
Force transferred to the inner shear key (kN)	–	18.7	44.7

Note: the value with asterisk in Table 5 shows the bending moment acting on the mid-depth of the end grain glulam cross-section in HBS at mid-span, due to the eccentricity of the resultant compressive force.

Table 6
Sensitivity analysis on the longitudinal position of the shear keys for HB.

		Deflection in glulam at mid-span (mm)					
		Location of the inner shear key					
		0.7 m	0.8 m	0.9 m	1.0 m	1.1 m	1.2 m
Location of the outer shear key	0.3 m	*26.8*	26.7	26.6	26.7	26.7	*26.8*
	0.4 m	–	26.7	26.7	26.7	26.7	*26.8*
	0.5 m	–	–	*26.8*	*26.8*	**26.8**	*26.9*
	0.6 m	–	–	–	*27.0*	*27.0*	*27.1*
	0.7 m	–	–	–	–	*27.3*	*27.3*
	0.8 m	–	–	–	–	–	*27.7*

0.9 m from the supports. The deflection under the reference shear key alignment (0.5 m and 1.1 m from the supports) is around average among all the studied cases in Table 6 for HB. Considering the slight difference of deflection between each case in Table 6, the position of the shear keys has a small influence on the stiffness of HB. On the other hand, a significant change of stiffness is observed when the position of the shear keys is changed in HBS, see Table 7. HBS reaches the minimum deflection at mid-span with a value of 35.0 mm when the inner shear key is 1.2 m and the outer shear key is 0.4 m or 0.5 m from the supports. The deflection under the reference shear key alignment is lower than most of the studied cases for HBS when the outer and inner shear keys are located from 0.3 m to 0.8 m and from 0.7 m to 1.1 m respectively.

In addition, the effect of the variation of the slip modulus of shear keys on internal forces and deflections for the hybrid beams is illustrated in Fig. 8. Significant variations of the structural response can be observed only within the range of the slip modulus from 5 kN/mm to 65 kN/mm, while after that all of the curves tend to reach a plateau. It is possible to observe that, within this range, the variation of the slip modulus has a much higher impact on the internal forces of HB than HBS. The opposite happens if deflections are analyzed, where it is possible to observe that the slip modulus has a high impact on serviceability behavior of HBS and almost a negligible one for HB.

Table 7
Sensitivity analysis on the longitudinal position of the shear keys for HBS.

		Deflection in glulam at mid-span (mm)					
		Location of the inner shear key					
		0.7 m	0.8 m	0.9 m	1.0 m	1.1 m	1.2 m
Location of the outer shear key	0.3 m	*43.3*	*41.2*	*39.3*	*37.7*	*36.3*	35.2
	0.4 m	-	*41.1*	*39.2*	*37.6*	*36.2*	35.0
	0.5 m	-	-	*39.2*	*37.6*	**36.2**	35.0
	0.6 m	-	-	-	*37.3*	*36.3*	35.1
	0.7 m	-	-	-	-	*36.5*	35.3
	0.8 m	-	-	-	-	-	35.6

Note: in Tables 6 and 7, values in bold represent the deflection under the reference shear key alignment, values in italic mean that they are larger than or equal to the deflection of the reference configuration and values with underline are smaller.

Furthermore, the effect of the axial stiffness of the rod on internal forces and deflections for both hybrid beams, i.e. HB and HBS was investigated by varying the rod diameter (Fig. 9). For HB it is possible to observe that the increase of the rod diameter determines higher forces acting on the rod and the shear keys, and this is due to the fact that the hybrid structural system (rod + glulam) works as a parallel system as compared to the simple glulam component, therefore the higher is the axial stiffness of the rod, the higher is the load taken by it. On the other hand, it is possible to observe that the increase of the diameter of the rod shifts the contribution of the absorption of the tensile force in the rod from the inner to the outer shear key. This fact can be explained through the analytical model proposed by Ref. [16]. Finally, the deflections significantly decrease for HBS when the diameter of the rod varies from 2 mm to around 14 mm, after which the deflection is almost constant. The effect of the increase of the rod diameter on deflection is much less important for HB.

(Please see online version for colors.)

3.4. Discussion of numerical results

From the comparison of bending moment diagrams on glulam for the three analyzed beam configurations (Fig. 7) it is possible to observe that its value is lower for the hybrid solutions (HB and HBS) with respect to the pure glulam case (SGB). This beneficial effect on glulam components is due to the localized bending moments transferred from the shear keys because of the eccentricity between internal compressive and tensile forces acting on the glulam element and rod, respectively. The reduction effect is proportional to the axial force percentage taken by each shear key.

For the considered load and geometrical configurations, the highest bending moment in glulam for HBS takes place around the inner shear key. Therefore, both the section at the inner shear key with the highest bending moment and the one at mid-span with the highest axial force should be checked for the combined compression and bending moment actions. However, it is not the common rule for all types of HBS. For HBS with different configurations it could be possible that the highest axial force and bending moment act on the same section, or there might even appear a negative moment to make the beam concave downwards if the reduction effect on the bending moment is significant. Analysis should be conducted for each individual case. Moreover, it is shown in Table 5 that for the analyzed configuration of HBS the maximum deflection in the rod is approximately 12 mm lower than the deflection in glulam at mid-span. It implies that there may be contact between the glulam beam and steel rod. This behavior would offer additional resistance thanks to second-order effects but is not considered in this study because of difficulties in its correct prevision.

From the sensitivity analysis of shear key location (Tables 6 and 7) it resulted that this parameter has a limited influence on the stiffness of HB while the influence is more important for HBS. Meanwhile, the minimum deflection of glulam at mid-span shows up under different shear key alignments for HB and HBS. For the latter type of beam, it is found that, for a fixed location of the outer shear key, the deflection tends to decrease with the increase of the distance of the two shear keys. For a fixed location of the inner shear key, the deflections of glulam at mid-span when the outer shear key is located at 0.4 m or 0.5 m from the supports, are smaller than those when the outer shear key is located at other positions (0.3 m, 0.6 m, 0.7 and 0.8 m from the support).

From the sensitivity analysis of the slip modulus of the shear keys (Fig. 8) it resulted that for low values of this parameter the external load is mainly taken by the bending moment of glulam component in

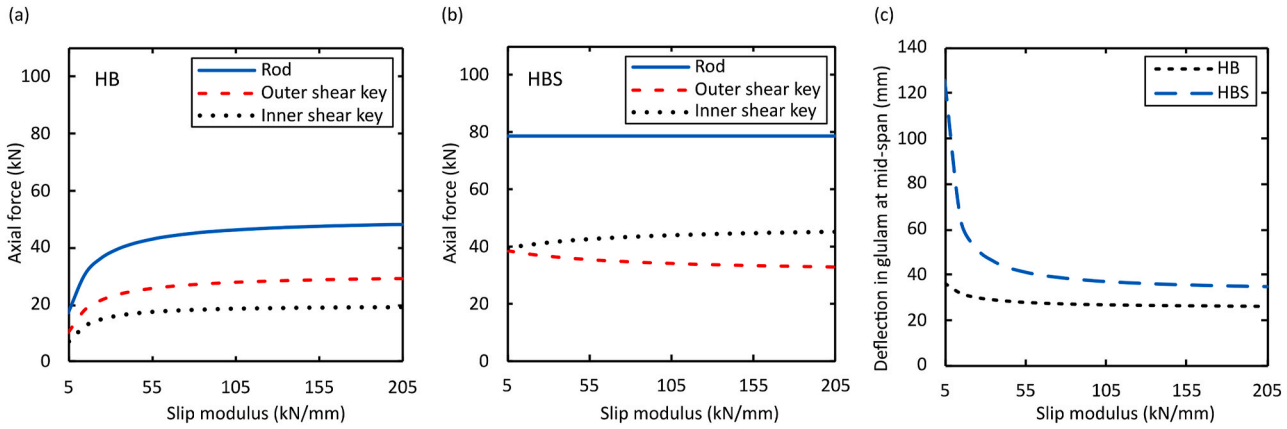

Fig. 8. Sensitivity analysis of slip modulus of shear key: effect on internal axial force for (a) HB and (b) HBS, and (c) effect on deflection of glulam component for HB and HBS.(Please see online version for colors.)

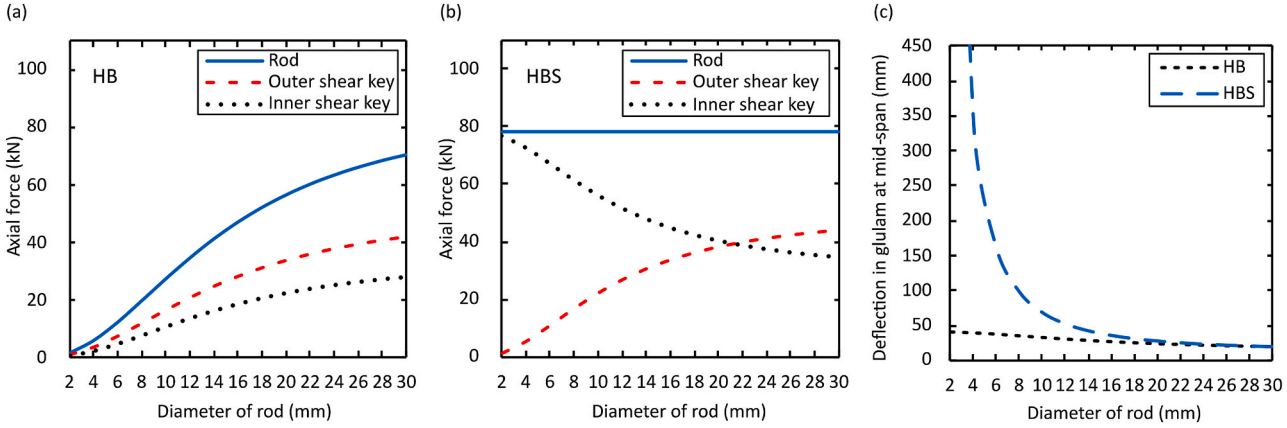

Fig. 9. Sensitivity analysis of diameter of the rod: effect on internal axial force for (a) HB and (b) HBS, and (c) effect on deflection of glulam component for HB and HBS.

HB, and it is due to the fact that the glulam member and the composite action work as parallel systems.

For HBS, the slighter influence on the force distribution among the shear keys to the variation of the slip modulus is due to the fact that the entity of shear taken by each shear connection is not only the function of the slip modulus. Actually, given that the distribution of the axial force acting on the rod as shear forces on the outer and inner shear keys is the function of their axial stiffness, $k_{ex}$and k_{in}, it is possible to observe from (10) and (11) that the slip modulus of shear keys is only one of the contributions that determine their values:

$$\frac{1}{k_{ex}} = \frac{1}{k_{T,ex}} + \frac{1}{k_{ser}} + \frac{1}{k_b} + \frac{1}{k_{a,ex}} \tag{10}$$

$$\frac{1}{k_{in}} = \frac{1}{k_{T,in}} + \frac{1}{k_{ser}} + \frac{1}{k_{a,in}} \tag{11}$$

where $k_{T,ex}$ and $k_{T,in}$ are the translational stiffnesses associated to the rotational stiffness of glulam component at the sections placed at outer and inner shear keys respectively; k_{ser} is the slip modulus of shear key; k_b is the axial stiffness of rod; $k_{a,ex}$ and $k_{a,in}$ are the axial stiffnesses of glulam component taken a segment comprised between the outer and inner shear keys respectively [16].

Mathematically, the value of k_{ex} and k_{in} in (10) and (11) are both mainly determined by the minimum of addends on the right side of the equation. When the slip modulus is assumed with low values, it results in similar axial stiffness of the outer and inner shear key and leads to a nearly-equal force distribution as shown in Fig. 8.b. The variation of slip modulus does not influence the structural response significantly in terms of axial force and systematic stiffness when the slip modulus is over 65 kN/mm.

The third sensitivity analysis studied the effect of the diameter of the rod on the structural response. From (10) and (11) it should be noted that, for HBS, stiffness of rod is one of the contributions that directly influence the axial force transferred to the outer shear key but not the inner one. Therefore, when the rod diameter is small, the contribution of the outer shear key on the axial force distribution is small if compared to the one of the inner shear key, leading to a high force transferred to the inner shear key as shown in Fig. 9.b. Lastly, deflection in HB decreases slightly with the increase of rod diameter from 2 mm to 30 mm while deflection in HBS starts to drop marginally as well when the rod diameter is above 14 mm, meaning that a rod diameter over 14 mm has limit effect on the stiffness of both hybrid beams.

3.5. Comparison between analytical and numerical results

Results obtained from numerical analysis show good agreement with the results from the analytical calculation. The displacement and secant stiffness under 10 kN external load at each one-third point are summarized in Table 8. It is noticed that, for HBS, there is a small difference of axial force between analytical and numerical results, which is due to the different assumptions (elasto-plastic and linear elastic behaviors of glulam were assumed in analytical and numerical models respectively) when calculating the position of neutral axis with regard to the compressive zone in glulam. For each type of beam, the displacement from the analytical calculation is slightly smaller than that from numerical analysis, which could be explained by the fact that the shear defor-

Table 8
Axial force in the rod, the maximum deflection and secant stiffness under 10 kN external load at each one-third point for each type of beam obtained from each method.

Type of beam	Method		Axial force in the rod (kN)	The maximum deflection in glulam (mm)	Secant stiffness (kN/mm)
SGB	Analytical		–	40.0	0.50
	Numerical		–	41.4	0.48
HB	Analytical	PC method	48.7	25.1	0.80
		γ method	47.0	25.1	0.80
	Numerical		47.1	26.8	0.74
HBS	Analytical		73.6	32.3	0.62
	Numerical		78.4	36.2	0.55

mation is neglected in the analytical calculation. By comparing the secant stiffness, it can be concluded that the hybrid beams, HBS and HB, are approximately 20% and 60% stiffer than SGB, respectively.

Moreover, the decreased cross-sectional area of glulam member around the notch is not considered in the analytical and numerical models described in Section 2.3 and 2.4. However, a further modification on the numerical models for the hybrid beams HB and HBS is carried out that assigns smaller cross section to glulam around the notch. It is found that the influence of the decreased cross-sectional area of glulam on the secant stiffness is negligible (only around 1% increasement of deflection in glulam for both HB and HBS under 10 kN external load at each one-third point). Furthermore, the interaction of localized stresses in glulam around the shear keys are neglected in the analytical models for the analysis of bearing capacities and failure modes. Hence, advanced 3D model and experimental investigations are planned in the future for comparison with the analytical results showed in this work.

4. Conclusions

In this paper an innovative system composed of steel shear-key connections and steel rods to create timber-steel hybrid (composite) members is presented. On the one hand, the system has proven by the analytical and numerical studies to be employable as retrofitting technique to considerably improve strength and stiffness performances of existing timber beams. On the other hand, it can be used to join short beams to create longer composite structural members, providing cost-saving in production, transportation and building-erection phases. Three types of beams were investigated through analytical and numerical models: the simple glulam beam (SGB), the hybrid beam without splice (HB) and the hybrid beam with a splice at mid-span (HBS). Two analytical methods, i.e. partial composite method and gamma method, were considered to study the behavior of the hybrid beam without splice. Stress and strain distributions for both types of hybrid beams were investigated to predict failure modes and bearing capacities. A parametric analysis to investigate the mechanical behavior related to the longitudinal position of the shear keys, the slip modulus of shear key connections and the diameter of rod was carried out for both types of hybrid beams through 2D numerical beam models. The main results are:

- for hybrid beam without splice (HB), the results obtained from partial composite method and gamma method show high similarities. Gamma method is therefore a reliable and simple analytical model to predict the mechanical behavior of this type of hybrid structure;
- results obtained from numerical analyses are in good agreement with the ones obtained from the analytical calculation. For all the types of beam the displacement predicted through the analytical models is slightly smaller than the one from the numerical analyses since the shear deformation contribution is neglected in the analytical calculation. For hybrid beam with splice (HBS), a small difference of the axial force between analytical and numerical models is attributed to the different assumptions when calculating the position of neutral axis regarding the compressive zone in glulam;
- the hybrid beams with (HBS) and without (HB) splice are approximately 20% and 60% stiffer than the simple glulam beam (SGB) in the elastic stage, respectively. Thus, the proposed innovative shear-key system can be used to create timber-based hybrid structural elements that, once properly designed, can efficiently improve the stiffness to vertical loads respect to traditional simple glulam beams;
- according to the analytical calculations, both hybrid beam typologies show ductile behaviors and higher bearing capacities (yielding of glulam in compression parallel to the grain for the hybrid beam without splice (HB) and yielding of rod for the hybrid beam with a splice at mid-span (HBS) when the single load is 14.8 kN and 16.5 kN, respectively) compared to the simple glulam beam (SGB) with brittle bending failure when the load is 13.9 kN at each one-third point;
- the stiffness of the hybrid beam with splice (HBS) is more sensitive to the three mechanical parameters, i.e. the longitudinal positions of the shear keys, the slip modulus of the shear key connection and the diameter of rod, than the hybrid beam without splice (HB);
- the shear key locations have a small influence on the stiffness of the hybrid beam without splice (HB) while the influence is more significant for the hybrid beam with splice (HBS). The minimum deflection takes place under different shear key alignments for the hybrid beams with (HBS) and without (HB) splice. The deflection with the reference shear key alignment (0.5 m and 1.1 m for the outer and inner shear keys from the supports) is around average among all the studied cases (the outer and inner shear keys from 0.3 m to 0.8 m and from 0.7 m to 1.2 m with an interval of 0.1 m respectively) for the hybrid beam without splice (HB). However, for the hybrid beam with splice (HBS), the deflection with the reference shear key alignment is smaller than most of the studied cases when the inner shear keys are located from 0.7 m to 1.1 m from the supports;
- the variation of slip modulus does not influence much the structural response of the hybrid beams if the assumed value of slip modulus for timber-steel connection is not lower than 135 kN/mm. In order to obtain a more accurate value, further investigations on this parameter will be carried out both with advanced numerical analyses and experimental tests;
- the third parametric study shows that, for the hybrid beam without splice (HB), the increase of rod diameter determines higher force in the rod and shear keys, while for the hybrid beam with splice (HBS), the contribution of the inner and outer shear keys on the tensile force distribution shifts dramatically with the increase of rod diameter. When the rod diameter is over 14 mm, its effect on the structural stiffness is limited for both types of hybrid beams.

Future developments will include both static tests to compare the results herein reported with an experimental dataset as well as dynamic tests to determine vibration behavior and damping properties of the proposed novel hybrid system. In addition, a configuration with post-tensioned rods will be tested and the load-displacement behavior of notched timber-steel connections will be investigated through local tests. Parametric analyses related to different geometrical and load configurations will also be carried out. The innovative timber-steel hybrid beams could be further improved in terms of fire resistance performance. Unprotected steel reduces the stiffness and strength more quickly when it is exposed to high temperature compared to timber. Thus insulation, e.g. by means of a box-like lamination made of the same timber material as the beam itself, is suggested to cover the steel

components in real connection and retrofitting applications. Moreover, it is worth mentioning that uplift force could be taken by the hybrid beam without splice (HB) while the hybrid beam with splice (HBS) has limited load-carrying capacity in case of uplift forces. The latter solution should therefore be used with caution in situations where the permanent loads are small and there is a risk for uplift forces, e.g. in light roof structure.

Credit author statement

Tianxiang Wang: Conceptualization, Methodology, Software, Validation, Visualization, Writing – original draft, Formal analysis, Investigation. Yue Wang: Conceptualization, Methodology, Software, Validation, Visualization, Writing – original draft, Formal analysis, Investigation. Roberto Crocetti: Conceptualization, Methodology, Project administration, Supervision, Writing – review & editing. Luca Franco: Conceptualization, Methodology, Investigation, Validation, Writing – review & editing. Michael Schweigler: Software, Validation, Supervision, Writing – review & editing. Magnus Wålinder: Project administration, Supervision, Writing – review & editing.

Declaration of competing interest

The authors declare that they have no known competing financial interests or personal relationships that could have appeared to influence the work reported in this paper.

References

[1] B.H. Ahmadi, M.P. Saka, Behavior of composite timber-concrete floors, J. Struct. Eng. 11 (1993) 3111–3130, https://doi.org/10.1061/(ASCE)0733-9445(1993)119:11(3111).

[2] American Wood Council, National Design Specification for Wood Construction, AWC, Leesburg, USA, 2018 https://www.awc.org/pdf/codes-standards/publications/nds/AWC-NDS2018-ViewOnly-171117.pdf.

[3] B. Anshari, Z. Guan, Q. Wang, Modelling of Glulam Beams Pre-stressed by Compressed Wood, 2017, pp. 160–170, https://doi.org/10.1016/j.compstruct.2017.01.028.

[4] J. Balogh, M. Fragiacomo, R.M. Gutkowski, R.S. Fast, Influence of repeated and sustained loading on the performance of layered wood-concrete composite beams, J. Struct. Eng. 134 (3) (2008) 430–439, https://doi.org/10.1061/(ASCE)0733-9445(2008)134:3(430).

[5] A. Ceccotti, R. Fellow, M. Fragiacomo, S. Giordano, Long-term and collapse tests on a timber-concrete composite beam with glued-in connection, Mater. Struct. (10) (2006) 15–25 04, https://doi.org/10.1617/s11527-006-9094-z.

[6] R. Crocetti, Large-span timber structures, Proceedings of the World Congress on Civil, Structural, and Environmental Engineering, 2016 March 30-31, 2016, Prague, Czech Republic, https://doi.org/10.11159/icsenm16.124.

[7] R. Crocetti, M. Johansson, H. Johnsson, R. Kliger, A. Mårtensson, B. Norlin, A. Pousette, S. Thelandersson, Design of Timber Structures, Swedish Wood, Stockholm, Sweden, 2011 https://www.svenskttra.se/publikationer-start/publikationer/design-of-timber-structures/.

[8] J.F. Davalos, J.R. Loferski, S.M. Holzer, V. Yadama, Transverse isotropy modeling of 3-D glulam timber beams, J. Mater. Civ. Eng. 3 (2) (1991) 125–139, https://doi.org/10.1061/(ASCE)0899-1561(1991)3:2(125).

[9] A. Dias, J. Schänzlin, P. Dietsch, Design of Timber-Concrete Composite Structures, Shaker, Aachen, Germany, 2018 https://webarchiv.typo3.tum.de/TUM/costfp1402/fileadmin/w00btl/www/All_Members/Dias__A._Schaenzlin__J._Dietsch__P._Design_of_Timber-Concrete_Composite_Structures.pdf.

[10] M. Dorn, Investigations on the Serviceability Limit State of Dowel-type Timber Connections, Vienna University of Technology, Vienna, Austria, 2012 PhD dissertation http://lnu.diva-portal.org/smash/record.jsf?pid=diva2%3A800842&dswid=3169.

[11] D. Ed, F. Hasselqvist, Timber Compression Strength Perpendicular to the Grain - Testing of Glulam Beams with and without Reinforcement, Lund University, Lund, Sweden, 2011 Master dissertation http://lup.lub.lu.se/luur/download?func=downloadFile&recordOId=3159865&fileOId=3159867.

[12] EN 1995-1-1:2004, Eurocode 5: Design of Timber Structures, Common rules and rules for buildings. European Committee for Standarization, Brussels, Belgium, 2004 Part 1-1: General https://www.phd.eng.br/wp-content/uploads/2015/12/en.1995.1.1.2004.pdf.

[13] EN 1995-2:2004, Eurocode 5: Design of Timber Structures, European Committee for Standarization, Brussels, Belgium, 2004 Part 2: Bridges https://www.phd.eng.br/wp-content/uploads/2015/02/en.1995.2.2004.pdf.

[14] European Organization for Technical Assessment (EOTA), Rotho Blaas Self-tapping screws and threaded rods European Technical Assessment ETA-11/0030 2019. https://www.rothoblaas.com/ftp/ETA_11_0030_RB_screws_2019.pdf.

[15] M. Flaig, T. Schmidt, H.J. Blaß, Compressive strength and stiffness of end grain contact joints in glulam and CLT, Proceedings of the International Network on Timber Engineering Research (INTER) 2019 - Meeting, vol. 52, Tacoma, USA, 2019, pp. 313–325 August 26-29, 2019.

[16] L. Franco, Numerical Modelling Strategies and Design Methods for Timber Structures, Univiersity IUAV of Venezia, Venice, Italy, 2020 PhD dissertation.

[17] U.A. Girhammar, V.K.A. Gopu, Composite beam-columns with interlayer slip - exact analysis, J. Struct. Eng. 119 (4) (1993) 1265–1282, https://doi.org/10.1061/(ASCE)0733-9445(1993)119:4(1265).

[18] G. He, L. Xie, X. Wang, J. Yi, L. Peng, Z. Chen, P.J. Gustafsson, R. Crocetti, Shear Behavior Study on Timber-Concrete Composite Structures with Bolts. BioResources, 2016, pp. 9205–9218, https://doi.org/10.15376/biores.11.4.9205-9218.

[19] M. He, Z. Li, F. Lam, R. Ma, Z. Ma, Experimental investigation on lateral performance of timber-steel hybrid shear wall systems, J. Struct. Eng. (2014) 04014029, https://doi.org/10.1061/(ASCE)ST.1943-541X.0000855.

[20] JCSS, Probabilistic Model Code ParT 3: Resistance Models, 2006 s.l.: s.n. https://www.jcss-lc.org/publications/jcsspmc/timber.pdf.

[21] S. Källbom, Characterisation of Thermally Modified Wood for Use as Component in Biobased Building Materials PhD dissertation KTH Royal Institute of Technology, Stockholm, Sweden, 2018 urn:nbn:se:kth:diva-233569.

[22] N. Khorsandnia, H. Valipour, K. Crews, Structural response of timber-concrete composite beams predicted by finite element models and manual calculations, Adv. Struct. Eng. (2014) 1601–1621, https://doi.org/10.1260/1369-4332.17.11.1601.

[23] H.J. Larsen, J. Munch-Andersen, CIB-W18 timber structures, A Review of Meetings, 2011, pp. 1–43 http://cib-w18.com/sites/default/files/pdfs/2%20Materials.pdf.

[24] M. Leborgne, R. Gutkowski, Effects of various admixtures and shear keys in wood-concrete composite beams, Construction and Building Maretials (2010) 1730–1738, https://doi.org/10.1016/j.conbuildmat.2010.02.016.

[25] J. Miller, W. Bulleit, Analysis of mechanically laminated TImber beams using shear keys, J. Struct. Eng. (2011) 124–132, https://doi.org/10.1061/(ASCE)ST.1943-541X.0000273.

[26] D. Peñaloza, The Role of Biobased Building Materials in the Climate Impacts of Construction: Effects of Increased Use of Biobased Materials in the Swedish Building Sector PhD dissertation KTH Royal Institute of Technology, TRITA-BYMA 2017:02, Stockholm, Sweden, 2017, p. 50 urn:nbn:se:kth:diva-207130.

[27] J. Porteous, A. Kermani, Structural Timber Design to Eurocode 5, Blackwell Publishing Ltd, 2007 https://onlinelibrary.wiley.com/doi/book/10.1002/9780470697818.

[28] T. Schmidt, H.J. Blass, Recent development in CLT connections Part 1: in-plane shear connection for CLT bracing elements under static loads, Wood Fiber Sci. (2018) 48–57, https://doi.org/10.22382/wfs-2018-039.

[29] K.-U. Schober, T. Tannert, Hybrid connections for timber structures, European Journal of Wood and Wood Products (2016) 369–377 03 03, https://doi.org/10.1007/s00107-016-1024-3.

[30] C.P. Siess, I.M. Viest, N.M. Newmark, Studies of Slab and Beam Highway Bridges: Part III: Small-Scale Tests of Shear Connectors and Composite T-Beams, University of Illinois at Urbana Champaign, Urbana-Champaign, USA, 1952 http://hdl.handle.net/2142/4513.

[31] Standards Australia, Timber Structures Design Methods, SAI Global, Sydney, Australia, 2010 https://infostore.saiglobal.com/en-us/standards/as-1720-1-2010-126188_saig_as_as_274062/.

[32] T. Vallée, T. Tannert, S. Hehl, Experimental and numerical investigations on full-scale adhesively bonded timber trusses, Mater. Struct. (2011) 1745–1758 07 04, https://doi.org/10.1617/s11527-011-9735-8.

[33] D. Yeoh, M. Fragiacomo, M.D. Franceschi, K.H. Boon, State of the art on timber-concrete state of the art on timber-concretes structures: literature review, J. Struct. Eng. 137 (10) (2011) 1085–1095, https://doi.org/10.1061/(ASCE)ST.1943-541X.0000353.

[34] X. Zhang, M. Fairhurst, T. Tannert, Ductility estimation for a novel timber-steel hybrid system, J. Struct. Eng. (2016) E4015001, https://doi.org/10.1061/(ASCE)ST.1943-541X.0001296.